# Kinetic Study of Acid Hydrolysis of Corn Cob to Xylose

**B.N. Uzoh[1], O.E. Onyelucheya[1], J.C. Obijiaku[1,2]***

[1]Department of Chemical Engineering, Federal University of Technology,
P.M.B 1526, Owerri, Nigeria
[2]Ralph E. Martin Department of Chemical Engineering, University of Arkansas,
Fayetteville, AR 72701, United States of America (USA)

**ABSTRACT:** Corn cob is one of the common renewable, cheap and abundant lignocellulosic materials. As a potential source of fermentable sugars, corn cob can be used as a substrate for value added products such as xylitol. This research paper studied the production of xylose from corn cob using phosphoric and nitric acids at 130$^0$C, and acid concentrations of 1wt%, 2wt%, 3wt%, 4wt% and 5wt% respectively, and at time intervals of 18mins, 36mins, 54mins, 72mins and 90mins respectively. The substrate was characterized for the proximate constituents and the results show that corn cob has high hemicellulose content. Seaman model and the Two-fraction model were used in studying the kinetics of xylose concentration in the hydrolysates, and the Two-fraction model proved to have a better fit with $R^2$ equal to 1. A maximum concentration of 11.034mg/ml of xylose was produced when 3wt% $H_3PO_4$ was used as catalyst for the hydrolysis and at a time interval of 38mins, with 67% susceptibility to hydrolysis. While for the nitric acid hydrolysis, 10.859mg/ml of xylose was produced as the maximum concentration when 3wt% of $HNO_3$ was used, at a hydrolysis time interval of 6mins, with 52% susceptibility to hydrolysis. In Comparison, the results showed that the nitric acid was a more efficient catalyst for acid hydrolysis of corn cobs.

**KEYWORDS:** Corn cob, Acid hydrolysis, Xylose, Lignocellulose material, Seaman's model, Two-fraction model.

https://doi.org/10.29294/IJASE.9.1.2022.2539-2555 ©2022 Mahendrapublications.com, All rights reserved

## 1. INTRODUCTION

Many agricultural wastes are costless and renewable, and are widespread sources of useful chemicals in today's world. Even though in most cases the lignocellulosic materials are burned off (which is an application with very low added value with negative environmental impact), the lignocellulosic nature of these agricultural wastes still makes them suitable for processing chemicals with high added value end products [1].The chemical fractionation of lignocellulosic materials into products derived from their structural components (cellulose, hemicellulose and lignin) has turned out to be an attractive possibility which has led to an identified integral benefit to the feed stocks. And since the separation of the structural fractions will usually require the degradation of some of them, a possible first step in the process aimed at the fractionation of these lignocellulosic material scan then be based on the selective degradation of hemicelluloses by means of pre hydrolysis (conventionally carried out in an acidic media) or auto hydrolysis (where which water is reacted with the raw material). This process allows the production of soluble and valuable chemicals from hemicellulose materials, leaving a solid residue (known to be made up of cellulose and lignin) which can ordinarily be valorized by a further processing [2].

Corncob, an important agricultural residue from the corn processing industry, has received increasing attention worldwide due to its high carbohydrate contents and high energy densities. And it has been considered as one of the most suitable biomasses with potential for the production of various high value-added chemicals such as xylose [3].

Corn cob (the substrate utilized in this work), a waste from corn production is largely available in Nigeria. The worldwide production of corn is 785 million tons with Africa producing 6.5% and Nigeria being the largest African producer with nearly 8 million tons. The

***Corresponding Author: jude.obijiaku@futo.edu.ng**

**Received**: 15.06.2022 **Accepted**: 27.07.2022 **Published on**: 01.08.2022

structure of corn cob is composed of cellulose, hemicelluloses and lignin. Cellulose and hemicelluloses are polymers of sugars, and potential source of fermentable sugars [4].

Due to the increasing energy consumption and the obvious negative environmental impacts, many researchers have been inspired to explore renewable energy resources for the production of numerous materials, and abundant lignocellulosic biomass have been identified as a potential and sustainable alternative to fossil resources [5].

In the diversification of the use of global renewable energy through better alternative sources there is need to convert agricultural residue which are in abundance to useful products such as xylitol [6]. And acid hydrolysis has being the common method applied. Hence, this research work tends to determine between phosphoric and nitric acids which is preferable in the process of converting agricultural residual to useful products. Xylitol is a natural five carbon sugar that has attracted much attention recently because of its potential use as a natural food sweetener. There is then need to properly understand the application of the kinetic models which were used to explain the variation with time of the main product generated and the optimal yield of xylose.

Corn cob is rich in xylose among all other lignocellulosic materials, making it a potential source of value-added products. Therefore, the hydrolysis of corn cob could be a good alternative for xylose production which could further be broken down to xylitol. Moreover, economic interest in xylitol productions can be enhanced if the required xylose solutions can be obtained from the hydrolysis of low-cost lingo cellulosic wastes [7].

This research paper is focused on the study of the concentration of xylose yield during the acid hydrolysis of corn cob using both Phosphoric and Nitric acids ($H_3PO_4$ and $HNO_3$)at a constant temperature of 130$^0$c, for time intervals of 18mins, 36mins, 54mins, 72mins and 90mins and acid concentrations of 1wt%, 2wt%, 3wt%, 4wt% and 5wt % respectively, and to determine the rate constants and other kinetic parameters of the individual acid hydrolysis process and to maximize sugar production.

## 2.0 THEORITICAL BACKGROUND

### *2.1 Kinetic Study of Lignocellulosic Material with Acids*

### *2.1.1 Kinetic Modeling of Lignocellulosic Material*

Saeman and Two fraction models are the two kinetic models mostly proposed to investigate the acid hydrolysis of lignocellulosic materials by different researchers [4].

### *2.1.2 Saeman's Model*

The simplified models for the study of the kinetics of hydrolysis process using acids began with the work of Saeman for the hydrolysis of douglas fire wood using sulphuric acid [8]. In his research the hydrolysis of cellulose was studied establishing the following model:

$$\text{Cellulose} \longrightarrow \text{Glucose} \xrightarrow{K_2} \text{Decomposition products}$$

where $k_1$(min$^{-1}$) is the rate for release of glucose from cellulose and $k_2$ (min$^{-1}$) is rate for glucose decomposition. This model considers the hydrolysis of cellulose to release glucose that in severe conditions is decomposed.

Eken-Saracglu *et al*., [9] applied the Seaman's modes in their study done on kinetic comparative of hemicelluloses hydrolysis in corn cob and sun flower seed hull. The model was also applied in the works of Esther *et al.* [10], for the hydrolysis of the hemicelluloses fraction of wheat straw using sulphuric acid. Onyelucheya *et al*., [4] in their study on acid hydrolysis of cassava peel applied similar models. Liang *et al*. [11] in the effort to study the acid hydrolysis of corncobs to levulinic acid applied the Saeman's models. The models were helpful to da Costa Lopes & Łukasik [12] in their work on separation and recovery of a hemicellulose-derived sugar produced from the hydrolysis of biomass by an acidic ionic liquid. Also, Wang *et al*., [13] adopted the Saeman's models in their kinetic study on the hydrolysis of corncob residues to levulinic acid. And Yuan *et al*. [1] equally applied the models in their kinetics studies on the hydrolysis of hemicellulose.

The model of Saeman can therefore be generalized for any polymer as:

$$\text{Polymer} \xrightarrow{K1} \text{Monomer} \xrightarrow{K2} \text{Decomposition products}$$

The generalized polymer could be cellulose, hemicellulose, etc.

where $K_1$ = Rate of generation reaction and $K_2$ = Rate of decomposition reaction, and:

$$r_A = d\frac{C_A}{dt} = -k_1 C_A \qquad (2.1)$$

$$r_B = d\frac{C_B}{dt} = -k_1 C_A - K_2 C_B \qquad (2.2)$$

$$r_C = d\frac{C_C}{dt} = k_2 C_B \qquad (2.3)$$

where $C_A$ = Polymer concentration
$C_B$ = Monomer concentration
$C_C$ = Decomposition product concentration

From equation (2.1)

$$d\frac{C_A}{dt} = -k_1 C_A$$

$$\int_{CA_0}^{C_A} \frac{dC_A}{C_A} = -k_1 \int_0^t dt$$

$$In\frac{C_A}{CA_0} = -K_1 t$$

$$C_A = C_{A0} e^{-K_1 t} \qquad (2.4)$$

Where; $C_{A0}$ = Initial Polymer concentration

Substituting equation (2.1) into (2.2)

$$\frac{dC_B}{dt} = k_1 C_{A0} e^{-K_1 t} - k_2 C_B$$

$$\frac{dC_B}{dt} + k_2 C_B = k_1 C_{A0} e^{-K_1 t} \qquad (2.5)$$

Equation (2.5) can be solved by Laplace transform or integrating factors.

Applying Laplace transform to equation (2.5);

$$L\left[\frac{dC_B}{dt}\right] + k_2 L[C_B] = k_1 C_{A0} L[e^{-k_1 t}]$$

$$L\left[\frac{dC_B}{dt}\right] = -k_2 L[C_B] + k_1 C_{A0} L[e^{-k_1 t}]$$

$$sC_B(s) - C_B(0) = -k_2 C_B(s) + \frac{k_1 C_{A0}}{S + k_1}$$

$C_B(0) = 0$ Because there is no monomer yet at time 0 sec.

$$sC_B(s) = -k_2 C_B(s) + \frac{k_1 C_{A0}}{S + k_1}$$

$$sC_B(s) + k_2 C_B(s) = \frac{k_1 C_{A0}}{S + k_1}$$

$$C_B(s)[s + k_2] = \frac{k_1 C_{A0}}{[S + k_1]}$$

$$C_B(s) = \frac{k_1 C_{A0}}{(S + k_1)(S + k_2)} \qquad (2.6)$$

Resolve equation (2.6) into partial fraction

$$\frac{k_1 C_{A0}}{(S + k_1)(S + k_2)} = \frac{A}{(S + k_1)} + \frac{B}{(S + k_2)}$$

$$k_1 C_{A0} = A(s + k_2) + B(s + k_1)$$

Let s= - $k_1$

$$k_1 C_{A0} = A(k_2 - k_1)$$

$$A = \frac{k_1 C_{A0}}{(k_2 - k_1)} \qquad (2.7)$$

Let s = -$k_2$

$$k_1C_{A0} = A(-k_2 + k_2) + B(k_1 - k_2)$$

$$B = \frac{k_1C_{A0}}{(k_1-k_2)} \qquad (2.8)$$

$$C_B(s) = \frac{k_1C_{A0}}{(S+k_1)(S+k_2)} = \frac{k_1C_{A0}}{(k_2-k_1)(S+k_1)} + \frac{k_1C_{A0}}{(k_1-k_2)(S+k_2)} \qquad (2.9)$$

$$C_B(s) = \frac{k_1C_{A0}}{(k_2-k_1)(s+k_1)} - \frac{k_1C_{A0}}{(k_2-k_1)(s+k_2)}$$

$$C_B(s) = \frac{k_1C_{A0}}{(k_2-k_1)}\left[\frac{1}{(s+k_1)} - \frac{1}{(s+k_2)}\right] \qquad (2.10)$$

Find the Laplace inverse of equation (2.10)

$$C_B(t) = \frac{k_1C_{A0}}{(k_2-k_1)}\left[e^{-k_1t} - e^{-k_2t}\right] \qquad (2.11)$$

where; t = time

$C_{A0}$ can be determined analytically by equation (2.12)

$$C_{A0} = \frac{FZ\rho}{WSR} \qquad (2.12)$$

Where;

F= stoichiometric factor due to hydration of molecule during the hydrolysis

ρ= density of hydrolysate

z = composition of the raw material for the polysaccharides

WSR = water to solid ratio.

### 2.1.3 Two Fraction Model

Due to the limitation of Saeman's model to only one fraction of the polymer there was need to get an alternative called the Two fraction model which considered a susceptible or fast fraction and a less susceptible or slow fraction, as applied in the works of Aguilar *et al*. [14] and da Costa Lopes &Lukasik [12], where the Two fraction kinetic model showed a better fit as compared to the Saeman's model.

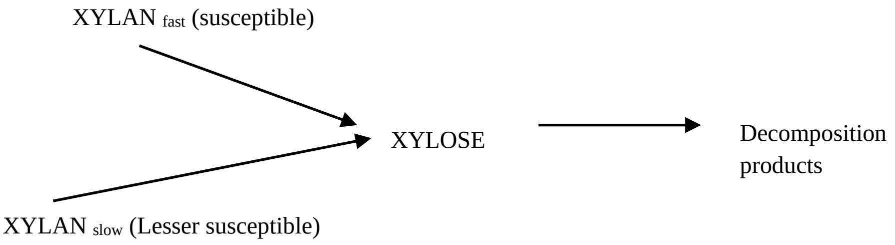

(2.13)

The ratio between the two fractions is the measured for the parameter ∝ which is the mass fraction of the susceptible polymer in the raw material as shown in equation (2.14):

$$\propto = \frac{\text{fast xylan}}{\text{total xylan}} \qquad (2.14)$$

The lesser susceptible fraction does not react, remaining always in the solid phase. Then the equation that governs the kinetics is;

$$\mathrm{C_B(t)} = \frac{\propto \mathrm{k_1C_{A0}}}{(\mathrm{k_2-k_1})}\left[\mathrm{e^{-k_1t} - e^{-k_2t}}\right] \qquad (2.15)$$

### 2.2 Comparing the Kinetic Parameters Based on Previous Research

### 2.2.1 Kinetic Modeling of Xylose Concentration

Xylose is the by-product obtained in the acid hydrolysis of lignocellulosic materials. Xylose released is from Xylan rich hemicellulose component of lignocellulosic material [4,15,7].

$$\text{Xylan} \overset{k_1}{\rightarrow} \text{ xylose } \overset{k_2}{\rightarrow} \text{ furfural} \qquad (2.16)$$

$\mathrm{k_1}$ and $\mathrm{k_2}$ are the kinetic coefficients of the reaction of monomer (xylose) released and decomposition respectively, both having unit of reciprocal time.

A review of previous works that used similar substrate but different acids at constant temperature is given below:

Sara *et al.* [16] in their work, studied the hydrolysis of sugar cane bagasse using phosphoric acid at different concentration (2wt%, 4wt% and 6wt %). They applied the Saeman's model as follows:

$$C_B(t) = \frac{k_1 C_{A0}}{(k_2 - k_1)}\left[e^{-k_1 t} - e^{-k_2 t}\right] \qquad (2.11)$$

where;

$C_B(t)$= the concentration of xylose at anytime

$C_{A0}$ = the initial concentration of xylan, and was determined by equation (2.12)

$$C_{A0} = \frac{FZ\rho}{WSR}$$

$$C_{A0} = \frac{150}{132} \text{ x } \frac{20.6}{10} \text{ x } 10 = 23.4 g/l$$

The Saeman model (Eqn 2.11) fitted better than Two fraction model, as shown in Table 2.1 indicating kinetic parameters of the Saeman model for xylan and the statistical value $R^2$.

**Table 2.1: Results of the kinetic model fit of Saeman model for Xylan showing the values of the kinetic parameters [16]**

| Operation Set | $K_1 x10^3(min^{-1})$ | $K_2 x10^3(min^{-1})$ | $R^2$ |
|---|---|---|---|
| 2% $H_3PO_4$at $122^0C$ | 3.64 | 1.12 | 0.98 |
| 4% $H_3PO_4$ at$122^0C$ | 5.89 | 1.92 | 0.96 |
| 6% $H_3PO_4$ at $122^0C$ | 7.36 | 3.52 | 0.97 |

The values of $k_1$ and $k_2$ increased with acid concentration. The values of $k_1$ are higher than those for $k_2$, but the ratio $k_1/k_2$ decreased with the time. Values of $k_1/k_2$ were 3.3, 3.1 and 2.1 for acid concentrations of 2%, 4% and 6%, respectively, indicating that the decomposition reactions of xylose are more important using higher acid concentration.

Aguilar *et al.*, [14] in their work carried out a kinetic study of the acid hydrolysis of sugar cane bagasse, using sulphuric acid at similar concentration (2wt%, 4wt% and 6wt %). They applied the fitting of the experimental data to both Saeman's model and two fraction models. According to the fitting of the Seaman's model (Eqn 2.11), the model was not good enough. This made them to modify the model to include the existence of two hemicellulose fractions as explained by Lavarack *et al.*, [17], in which one is easy (fast) to hydrolysis while the other is difficult (slow) to hydrolysis. The parameter $\propto$ represents the ratio between the fraction (g of susceptible xylan/g of total xylan) in the raw material. Equation (2.15) gives the modified form of Saeman's model and is called Two-fraction model.

$$C_B(t) = \frac{\propto k_1 C_{A0}}{(k_2 - k_1)}\left[e^{-k_1 t} - e^{-k_2 t}\right] \qquad (2.15)$$

Equation (2.15) gave a better fit compared to equation (2.11). It gave kinetic and statistical parameters of the fitting as shown in Table 2.2 below.

**Table 2.2: Kinetic and statistical parameters of xylose released for the $H_2S0_4$ hydrolysis of sugarcane bagasse [14]**

| Operation set | $\propto$(g/g) | $k_1(min^{-1})$ | $k_2 x10^3(min^{-1})$ | $R^2$ |
|---|---|---|---|---|
| 2% $H_2S0_4 at 122^0C$ | 0.973 | 0.1885 | 2.1 | 0.996 |
| 4% $H_2S0_4 at 122^0C$ | 0.998 | 0.1381 | 3.3 | 0.998 |
| 6% $H_2S0_4 at 122^0C$ | 0.933 | 0.2271 | 4.0 | 0.986 |

In their comparison of $k_1$ with $k_2$, it was observed that the kinetic coefficient of generation reactions of xylose are 80 fold higher than those of degradation reactions. Also comparing their work with Sara *et al.* [16], in treatments using nitric acid, the values of $k_1$ were slightly higher; while the values of $k_2$ were similar (the ratio $k_1/k_2$ was in the range 48–90).

Comparing these ratios, it can be deduced that the decomposition reactions of xylose are faster using phosphoric acid.

Some researchers also applied both models on their kinetic modeling of Xylose concentration. Esther *et al.*, [10] in their study of the kinetics of acid hydrolysis of wheat straw using sulphuric acid compared the Saeman's model and Two fraction model, and discovered that Two-fraction model gives a better fit than Saeman's model. The kinetic and statistical parameters of xylose released for the sulphuric acid hydrolysis of wheat straw at 130⁰C is given in Table 2.3.

**Table 2.3: Kinetic and statistical parameter for the hydrolysis of wheat straw using two-fraction model [10]**

| **Operational set** | $\propto_X\ (kgkg^{-1})$ | $X_0(K_gm)^{-3}$ | $k_1(min^{-1})$ | $k_2(min^{-1})$ | $r^2$ | $F - testprob$ |
|---|---|---|---|---|---|---|
| 1% $H_2S0_4$ | 0.634 | 7.55 | 0.1068 | 0.00026 | 0.9932 | 0.9930 |
| 2% $H_2S0_4$ | 0.294 | 14.22 | 0.1122 | 0.00124 | 0.9738 | 0.9736 |
| 3% $H_2S0_4$ | 0.227 | 16.10 | 0.1139 | 0.00302 | 0.9942 | 0.9852 |
| 4% $H_2S0_4$ | 0.193 | 16.18 | 0.1173 | 0.00389 | 0.9903 | 0.9929 |
| 5% $H_2S0_4$ | 0.182 | 16.32 | 0.1232 | 0.00494 | 0.9909 | 0.9937 |

$X_0$ is the initial concentration of Xylose determined by regression in $kgm^{-3}$. They compared the value of $k_1$ and $k_2$ and reached the conclusion that the kinetic coefficients of generation reaction of xylose are around 30fold higher than those of the degradation reactions. They realized also that, the values of kinetic coefficient increase with the concentration of catalyst though $k_1$ is lightly affected and $k_2$ strongly affected.

Antonio *et al.*, [18] carried out similar research work, on hydrolysis of sugarcane bagasse using nitric acid. In their research work they applied both models, and concluded that Two-fraction model was better because the statistical parameter ($R^2$) for Two-fraction model is closer to 100% compared to Saeman's model as shown in Table 2.4.

**Table 2.4: Result of the fitting for xylose concentration in the hydrolysis of sugarcane bagasse with nitric acid [18]**

| **Operational set** | **Saeman's model** | | | **Two-fraction model** | | | |
|---|---|---|---|---|---|---|---|
| | $k_2x10^3$ $(min^{-1})$ | $k_1$ $(min^{-1})$ | $R^2$ | $\propto_X$ (g/g) | $k_1(min^{-1})$ | $k_2x10^3$ $(min^{-1})$ | $R^2$ |
| 2% $HN0_3 at 100^0C$ | 3.9 | 0.006 | 0.952 | 0.40 | 0.0292 | 0.0 | 0.940 |
| 4% $HN0_3 at 100^0C$ | 2.6 | 0.021 | 0.770 | 0.57 | 0.098 | 0.0 | 0.973 |
| 6% $HN0_3 at 100^0C$ | 3.0 | 0.035 | 0.809 | 0.65 | 0.170 | 0.6 | 0.995 |
| 2% $HN0_3 at 122^0C$ | 1.7 | 0.033 | 0.902 | 0.77 | 0.102 | 0.4 | 0.964 |
| 4% $HN0_3 at 122^0C$ | 1.3 | 0.060 | 0.972 | 0.83 | 0.529 | 0.0 | 0.989 |
| 6% $HN0_3 at 122^0C$ | 3.1 | 0.074 | 0.937 | 0.80 | 0.695 | 1.1 | 0.998 |
| 2% $HN0_3 at 128^0C$ | 0.6 | 0.033 | 0.927 | 0.85 | 0.260 | 0.0 | 0.999 |
| 4% $HN0_3 at 128^0C$ | 0.9 | 0.98 | 0.964 | 0.84 | 0.978 | 0.0 | 0.999 |
| 6% $HN0_3 at 128^0C$ | 1.5 | 0.053 | 0.817 | 0.81 | 1.77 | 0.4 | 0.998 |

They assumed there was a total conversion of xylan to xylose. They concluded that $k_1$ increased with temperature and the acid concentration while the values of $k_2$ were zero or close to zero, which implies that the rate of xylose released was high and the degradation reaction negligible or very slow. Also, they concluded in their work that the parameter ∝increased with temperature, having an average value of 0.54g/g at 100⁰C, 0.80g/g at 122⁰C and 0.83g/g at 128⁰C.

## 3.0 MATERIALS AND METHOD

### *3.1 Material acquisition*

The corn cobs used for the experiments were gathered from local farmers in Obodoukwu Community in Ideato North LGA of Imo State, Nigeria. The fresh corn cobs (as shown in Fig

3.1) were gathered, sun dried for about three days, to effectively reduce the moisture content and surface wetness of the raw sample.

**Figure 3.1: Fresh corn cobs undergoing sun drying**

## *3.2 Pretreatment of Fresh Corn Cobs*

After the fresh corn cobs were sun-dried, they were taken to the grinding machine for particle size reduction to powdered form. The ground corn cobs (hydrolysis substrate) were then taken to laboratory, screened through a 1.0 mm mesh size, as shown in Fig 3.2, and stored in a container in a cool dry place, from where samples were taken and analyzed to determine some proximate parameters cellulose, hemicellulose, lignin, ash, carbohydrate and the moisture content.

**Figure 3.2: Screened Corn Cobs**

## *3.3 Acid Hydrolysis of the Corn Cobs*

20g of the sample (substrate) was weighed into a 500ml conical flask (reaction vessel). 400ml of phosphoric acid solution ($H_3PO_4$) was then added and the mixture swirled carefully, placed on an electro-thermal magnetic stirrer, set at 150rpm and at a temperature of 130$^0$C and at the pre-chosen time. At the end of the reaction time, the reaction mixture was quenched in a very cold ice-bath. After 2minutes, the content of the conical flask was filtered and labeled appropriately (with regards to reaction time conditions) and kept in a safe place for the xylose tests. The filtrate samples were afterwards taken to the UV-Spectrophotometer for the absorbance readings, at a wavelength of 554nm. For the filtrate sample preparations, Phloroglucinol Assay was used as outlined in the standard analytical procedures [11].

The same procedure was used for the nitric acid ($HNO_3$) hydrolysis and reducing sugar test preparations, at different operating time conditions of 18, 36, 54, 72 and 90minutes respectively at a temperature of 130$^0$C, using five different acid concentrations of 1%w/w, 2%w/w, 3%w/w, 4%w/w and 5%w/w respectively.

## *3.4 Calibration of Absorbance Reading*

0.1g of D-Xylose is dissolved in 100ml of standard benzoic acid to get a stock solution concentration of 10mg/ml. 0.5, 2.0, 4.0, 6.0 and 8.0ml were taken with the aid of a pipette into six test tubes. A test tube containing blank solution was also prepared. 9.5ml, 8.0ml, 6.0ml, 4.0ml, 0.5ml, and 2.0ml of distilled water were added to each test tube. Afterwards, 5µl of the prepared xylose standard solutions (and same in the case of the filtrate samples) were pipette into test tubes and 5ml of color reagent (Phloroglucinol Assay reagent) were added, covered with aluminum foil, and the test tubes taken to the hot water bath (at 100$^0$C) to heat for 4minutes. After 4minutes it was cooled and kept for the determination of the absorbance readings at a wavelength of 554 nm, for xylose at the different concentrations.

All experiments were carried out in duplicates and their average values were used to obtain the concentration values, from the xylose standard calibration curves.

## *3.5 Procedure for Absorbance Readings*

The spectrophotometer was switched on and allowed to boot for 30mins before use. The equipment was set to the measuring wavelength (for the sample) of the transmitting light and at 100% transmittance. The cuvettes where cleaned and filled to 4ml of the blank solution, and was inserted into the equipment to calibrate the machine at the set wavelength for that sample, with the blank solution. The blank solution was removed and in turn the cuvette was filled with the sample solutions and insert into the machine to obtain the absorbance readings for the sample solutions, at the set wavelength.

### *3.6 Procedure for Obtaining the Kinetic and Statistical Parameters*

The experimental results were converted from absorbance (nm) to concentrations with the aid of the calibration data given.

The concentration values were plotted against time (in minutes). The experimental data were fit to both kinetic models (Saeman & Two fraction) for phosphoric acid and nitric acid with a curve fitting tool in MatLab software, to obtain kinetic parameters ($k_1$and$k_2$), $\propto$ and statistical parameter (Adjusted $R^2$). where $k_1$ is the rate of monomer generation reaction, $k_2$ is the rate of monomer decomposition reaction while $\propto$ is the mass ratio of susceptible polymer fraction to total polymer (kg kg_1).

**Table 4.1: Main component of corn cob used in this study**

| Components | Mass fraction (%) |
|---|---|
| Hemicellulose | 42.36 |
| Cellulose | 31.26 |
| Lignin | 12.25 |
| Ash | 1.85 |
| Carbohydrate | 2.86 |
| Moisture content | 3.35 |
| Others | 6.07 |

## 4.0 RESULTS AND DISCUSSION

### *4.1 Results presentation*

The composition of the corn cob used in this study is shown in Table 4.1. The main fractions of corn cob were in the same range as other herbaceous materials, such as rice, wheat straw and sorghum straw.

To obtain relationship between absorbance and concentration with the aid of curve fitting tool in excel, the absorbance (nm) values were plotted against concentration (mg/dl) values shown in Table 4.2 to obtain the standard calibration curve.

**Table 4.2: Calibration data for xylose (554nm)**

| Absorbance (nm) | Concentration (mg/dl) |
|---|---|
| 0.00 | 0.000 |
| 0.50 | 0.012 |
| 2.00 | 0.016 |
| 4.00 | 0.022 |
| 6.00 | 0.036 |

#### *4.1.1 Experimental Result for Xylose Using Phosphoric Acid*

The experimental results of xylose concentration after conversion of its absorbance reading for phosphoric acids are given in Tables 4.3, 4.4, 4.5, 4.6, and 4.7.

**Table 4.3 Experimental result for the xylose released at 1wt% phosphoric acid**

| Time (min) | $G_1$ (nm) | $G_2$(nm) | $G_{average}$ (nm) | G (mg/ml) |
|---|---|---|---|---|
| 0 | 0 | 0 | 0 | 0 |
| 18 | 0.0541 | 0.0529 | 0.0535 | 8.780 |
| 36 | 0.0658 | 0.0650 | 0.0654 | 10.71 |
| 54 | 0.0608 | 0.0608 | 0.0608 | 9.964 |
| 72 | 0.0449 | 0.0457 | 0.0453 | 7.431 |
| 90 | 0.0477 | 0.0481 | 0.0479 | 7.855 |

**Table 4.4 Experimental result for the xylose released at 2wt% phosphoric acid**

| Time (min) | $G_1$ (nm) | $G_2$(nm) | $G_{average}$ (nm) | G (mg/ml) |
|---|---|---|---|---|
| 0 | 0 | 0 | 0 | 0 |
| 18 | 0.0562 | 0.0566 | 0.0564 | 9.243 |
| 36 | 0.0510 | 0.0518 | 0.0514 | 8.422 |
| 54 | 0.0497 | 0.0509 | 0.0503 | 8.250 |
| 72 | 0.0393 | 0.0393 | 0.0393 | 6.435 |
| 90 | 0.0371 | 0.0367 | 0.0369 | 6.062 |

**Table 4.5 Experimental result for the xylose released at 3wt% phosphoric acid**

| Time (min) | $G_1$ (nm) | $G_2$(nm) | $G_{average}$ (nm) | G (mg/ml) |
|---|---|---|---|---|
| 0 | 0 | 0 | 0 | 0 |
| 18 | 0.0588 | 0.0634 | 0.0611 | 10.01 |
| 36 | 0.0602 | 0.0602 | 0.0602 | 9.876 |
| 54 | 0.0619 | 0.0615 | 0.0617 | 10.11 |
| 72 | 0.0526 | 0.0520 | 0.0523 | 8.570 |
| 90 | 0.0552 | 0.0552 | 0.0552 | 9.042 |

**Table 4.6 Experimental result for the xylose released at 4wt% phosphoric acid**

| Time (min) | $G_1$ (nm) | $G_2$(nm) | $G_{average}$ (nm) | G (mg/ml) |
|---|---|---|---|---|
| 0 | 0 | 0 | 0 | 0 |
| 18 | 0.0602 | 0.0612 | 0.0607 | 9.952 |
| 36 | 0.0525 | 0.0533 | 0.0529 | 8.673 |
| 54 | 0.0482 | 0.0480 | 0.0481 | 7.881 |
| 72 | 0.0413 | 0.0413 | 0.0413 | 6.766 |
| 90 | 0.0328 | 0.0334 | 0.0331 | 5.428 |

**Table 4.7 Experimental result for the xylose released at 5wt% phosphoric acid**

| Time (min) | $G_1$ (nm) | $G_2$(nm) | G $_{average}$ (nm) | G (mg/ ml) |
|---|---|---|---|---|
| 0 | 0 | 0 | 0 | 0 |
| 18 | 0.0549 | 0.054 | 0.0548 | 8.99 |
| 36 | 0.0532 | 0.053 | 0.0533 | 8.74 |
| 54 | 0.0581 | 0.058 | 0.0581 | 9.53 |
| 72 | 0.0520 | 0.051 | 0.0517 | 8.47 |
| 90 | 0.0522 | 0.052 | 0.0521 | 8.54 |

Where;
$G_1$ = First absorbance reading
$G_2$ = Second absorbance reading
$G$ = Concentration of xylose in mg/ml

The kinetic and statistical parameter of xylose released, applying both Seaman's model and Two-fraction model using phosphoric acid is shown in Tables 4.8 & 4.9 below.

**Table 4.8 Kinetic and statistical parameter of xylose released for Seaman's model using phosphoric acid**

| Conc (wt%) | $K_1$ $(min^{-1})$ | $K_2$ $(min^{-1})$ | $AdjR^2$ |
|---|---|---|---|
| 1 | 0.0510 | 0.01152 | 0.9106 |
| 2 | 0.0547 | 0.01604 | 0.8409 |
| 3 | 0.0558 | 0.00991 | 0.9363 |
| 4 | 0.0657 | 0.01631 | 0.8535 |
| 5 | 0.0437 | 0.01082 | 0.9239 |

**Table 4.9 Kinetic and statistical parameter of xylose released for two fraction using phosphoric acid**

| Conc (wt%) | $K_1$ $(min^{-1})$ | $K_2$ $(min^{-1})$ | $\propto$ | $AdjR^2$ |
|---|---|---|---|---|
| 1 | 0.064 | 0.0092 | 0.899 | 0.9631 |
| 2 | 0.156 | 0.0069 | 0.668 | 0.9849 |
| 3 | 0.171 | 0.0024 | 0.675 | 0.9844 |
| 4 | 0.192 | 0.0083 | 0.716 | 0.995 |
| 5 | 0.185 | 0.0011 | 0.589 | 0.9843 |

**Table 4.10 Comparison of the experimental data with the model at 1wt% phosphoric acid for the xylose released**

| Time (min) | Experimental Data (mg/ml) | Saeman's Model (mg/ml) | Two-fraction model (mg/ml) |
|---|---|---|---|
| 0 | 0 | 0 | 0 |
| 18 | 8.780 | 7.849 | 8.663 |
| 36 | 10.71 | 10.54 | 10.79 |
| 54 | 9.964 | 9.634 | 9.877 |
| 72 | 7.431 | 7.272 | 7.464 |
| 90 | 7.855 | 7.067 | 7.747 |

**Table 4.11 Comparison of the experimental data with the model at 2wt% phosphoric acid for the xylose released**

| Time (min) | Experimental Data (mg/ml) | Saeman's Model (mg/ml) | Two-fraction model (mg/ml) |
|---|---|---|---|
| 0 | 0 | 0 | 0 |
| 18 | 9.243 | 8.5169 | 9.2144 |
| 36 | 8.422 | 7.5640 | 8.6860 |
| 54 | 8.250 | 8.3551 | 8.2007 |
| 72 | 6.435 | 5.7044 | 6.3998 |
| 90 | 6.062 | 5.1892 | 6.0027 |

**Table 4.12 Comparison of the experimental data with the model at 3wt% phosphoric acid for the xylose released**

| Time (min) | Experimental Data (mg/ml) | Saeman's Model (mg/ml) | Two-fraction model (mg/ml) |
|---|---|---|---|
| 0 | 0 | 0 | 0 |
| 18 | 10.013 | 9.1659 | 10.003 |
| 36 | 9.876 | 9.0259 | 10.024 |
| 54 | 10.112 | 10.354 | 9.6079 |
| 72 | 8.570 | 7.1966 | 8.4898 |
| 90 | 9.042 | 7.8589 | 8.7892 |

**Table 4.13 Comparison of the experimental data with the model at 4wt% phosphoric acid for the xylose released**

| Time (min) | Experimental Data (mg/ml) | Saeman's Model (mg/ml) | Two-fraction model (mg/ml) |
|---|---|---|---|
| 0 | 0 | 0 | 0 |
| 18 | 9.952 | 9.3629 | 9.9385 |
| 36 | 8.673 | 9.8499 | 8.8695 |
| 54 | 7.881 | 8.2232 | 7.6432 |
| 72 | 6.766 | 6.4005 | 6.5781 |
| 90 | 5.428 | 4.8547 | 5.6612 |

**Table 4.14: Comparison of the experimental data with the model at 5wt% phosphoric acid for the xylose released**

| Time (min) | Experimental Data (mg/ml) | Saeman's Model (mg/ml) | Two-fraction model (mg/ml) |
|---|---|---|---|
| 0 | 0 | 0 | 0 |
| 18 | 8.991 | 7.8317 | 8.9678 |
| 36 | 8.741 | 10.012 | 9.1034 |
| 54 | 9.527 | 9.8646 | 9.4888 |
| 72 | 8.470 | 7.8585 | 8.4569 |
| 90 | 8.542 | 7.6276 | 8.5684 |

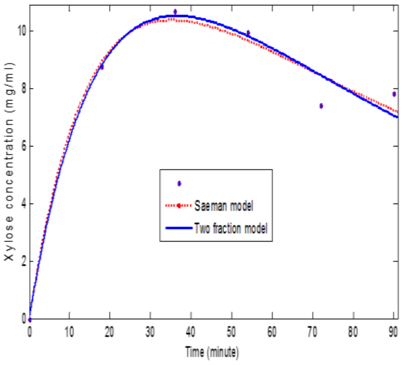

**Figure 4.1 The graph for xylose released at 1wt% phosphoric acid**

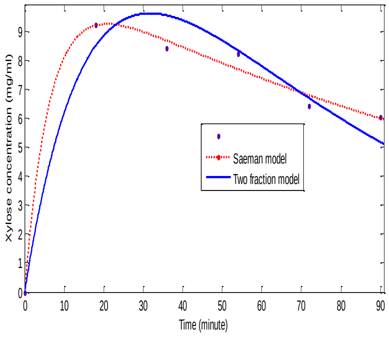

**Figure 4.2 The graph for xylose released at 2wt% phosphoric acid**

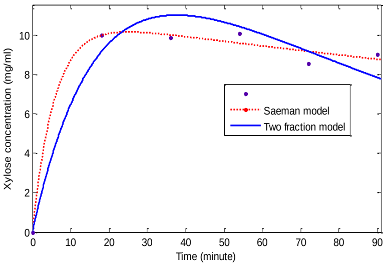

**Figure 4.3 The graph for xylose released at 2wt% phosphoric acid**

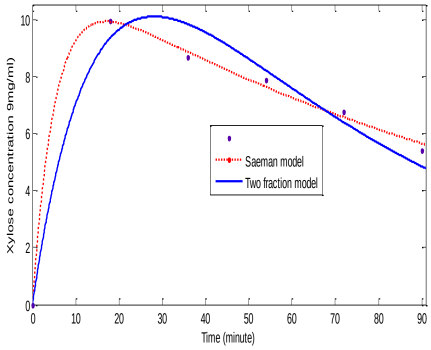

**Figure 4.4 The graph for xylose released at 4wt% phosphoric acid**

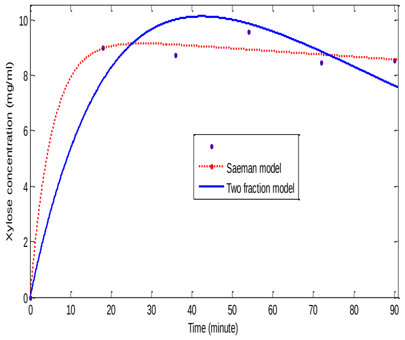

**Figure 4.5 The graph for xylose released at 5wt% phosphoric acid**

### *4.1.2 Experimental Result for Xylose Using Nitric Acid*

The experimental results of xylose concentration after conversion of its absorbance reading for nitric acids are given in Tables 4.15, 4.16 4.17, 4.18, and 4.19.

**Table 4.15 Experimental result for the xylose released at 1wt% nitric acid**

| Time (min) | $G_1$ (nm) | $G_2$(nm) | G $_{average}$ (nm) | G (mg/ml) |
|---|---|---|---|---|
| 0 | 0 | 0 | 0 | 0 |
| 18 | 0.0588 | 0.0606 | 0.0597 | 9.7913 |
| 36 | 0.0487 | 0.0488 | 0.0486 | 7.9672 |
| 54 | 0.0488 | 0.0486 | 0.0487 | 7.9836 |
| 72 | 0.0314 | 0.0314 | 0.0314 | 5.1475 |
| 90 | 0.0316 | 0.0312 | 0.0314 | 5.1475 |

*Uzoh et al.,*

**Table 4.16 Experimental result for the xylose released at 2wt% nitric acid**

| Time (min) | $G_1$ (nm) | $G_2$(nm) | $G_{average}$ (nm) | G (mg/ml) |
|---|---|---|---|---|
| 0 | 0 | 0 | 0 | 0 |
| 18 | 0.0567 | 0.0568 | 0.0568 | 9.3115 |
| 36 | 0.0623 | 0.0625 | 0.0624 | 10.2295 |
| 54 | 0.0550 | 0.0556 | 0.0553 | 9.0655 |
| 72 | 0.0441 | 0.0441 | 0.0441 | 7.2295 |
| 90 | 0.0496 | 0.0488 | 0.0492 | 8.0656 |

**Table 4.17 Experimental result for the xylose released at 3wt% nitric acid**

| Time (min) | $G_1$ (nm) | $G_2$(nm) | $G_{average}$ (nm) | G (mg/ml) |
|---|---|---|---|---|
| 0 | 0 | 0 | 0 | 0 |
| 18 | 0.0653 | 0.0657 | 0.0655 | 10.7377 |
| 36 | 0.0618 | 0.0610 | 0.0614 | 10.0656 |
| 54 | 0.0538 | 0.0538 | 0.0538 | 8.8196 |
| 72 | 0.0482 | 0.0482 | 0.0482 | 7.9016 |
| 90 | 0.0505 | 0.0509 | 0.0507 | 8.3115 |

**Table 4.18 Experimental result for the xylose released at 4wt% nitric acid**

| Time (min) | $G_1$ (nm) | $G_2$(nm) | $G_{average}$ (nm) | G (mg/ml) |
|---|---|---|---|---|
| 0 | 0 | 0 | 0 | 0 |
| 18 | 0.0640 | 0.0640 | 0.0640 | 10.4918 |
| 36 | 0.0593 | 0.0595 | 0.0594 | 9.7377 |
| 54 | 0.0543 | 0.0543 | 0.0543 | 8.9016 |
| 72 | 0.0527 | 0.0529 | 0.0528 | 8.6557 |
| 90 | 0.0485 | 0.0479 | 0.0482 | 7.9016 |

**Table 4.19 Experimental result for the xylose released at 5wt% nitric acid**

| Time (min) | $G_1$ (nm) | $G_2$(nm) | $G_{average}$ (nm) | G (mg/ml) |
|---|---|---|---|---|
| 0 | 0 | 0 | 0 | 0 |
| 18 | 0.0542 | 0.0544 | 0.0543 | 8.9016 |
| 36 | 0.0462 | 0.0462 | 0.0462 | 7.5736 |
| 54 | 0.0369 | 0.0371 | 0.0370 | 6.0656 |
| 72 | 0.0355 | 0.0355 | 0.0355 | 5.8197 |
| 90 | 0.0328 | 0.0330 | 0.0329 | 5.3934 |

Where;
$G_1$ = First absorbance reading
$G_2$ = Second absorbance reading
$G$ = Concentration of xylose in mg/ml

The Kinetic and statistical parameter of xylose released, applying both Seaman's model and Two-fraction model using nitric acid is shown in tables 4.20 & 4.21 below.

**Table 4.20 Kinetic and statistical parameter of xylose released for Seaman's model using nitric acid**

| Conc (wt%) | $K_1$ $(min^{-1})$ | $K_2$ $(min^{-1})$ | $AdjR^2$ |
|---|---|---|---|
| 1 | 0.04215 | 0.02685 | 0.8905 |
| 2 | 0.03637 | 0.01875 | 0.9151 |
| 3 | 0.03878 | 0.01799 | 0.8822 |
| 4 | 0.03878 | 0.01799 | 0.8822 |
| 5 | 0.0346 | 0.0283 | 0.8241 |

**Table 4.21 Kinetic and statistical parameter of xylose released for two fraction model using nitric acid**

| Conc (wt%) | $K_1$ $(min^{-1})$ | $K_2$ $(min^{-1})$ | $\propto$ | $AdjR^2$ |
|---|---|---|---|---|
| 1 | 0.2594 | 0.0095 | 0.530 | 0.953 |
| 2 | 0.1165 | 0.0054 | 0.535 | 0.961 |
| 3 | 0.8347 | 0.0038 | 0.521 | 0.998 |
| 4 | 0.7982 | 0.0038 | 0.521 | 0.998 |
| 5 | 0.9226 | 0.0075 | 0.462 | 0.982 |

**Table 4.22 Comparison of the experimental data with the model at 1wt% nitric acid for the xylose released**

| Time (min) | Experimental Data (mg/ml) | Saeman's Model (mg/ml) | Two-fraction model (mg/ml) |
|---|---|---|---|
| 0 | 0 | 0 | 0 |
| 18 | 9.7913 | 8.7257 | 9.7720 |
| 36 | 7.9672 | 6.4675 | 8.3246 |
| 54 | 7.9836 | 7.7524 | 7.8144 |
| 72 | 5.1475 | 4.6773 | 5.0996 |
| 90 | 5.1475 | 3.9210 | 4.9789 |

**Table 4.23 Comparison of the experimental data with the model at 2wt% nitric acid for the xylose released**

| Time (min) | Experimental Data (mg/ml) | Saeman's Model (mg/ml) | Two-fraction model (mg/ml) |
|---|---|---|---|
| 0 | 0 | 0 | 0 |
| 18 | 9.3115 | 8.5397 | 9.3908 |
| 36 | 10.229 | 9.5309 | 9.6713 |
| 54 | 9.0655 | 9.4201 | 8.9140 |
| 72 | 7.2295 | 7.1053 | 7.1728 |
| 90 | 8.0656 | 6.4775 | 7.3518 |

**Table 4.24 Comparison of the experimental data with the model at 3wt% nitric acid for the xylose released**

| Time (min) | Experimental Data (mg/ml) | Saeman's Model (mg/ml) | Two-fraction model (mg/ml) |
|---|---|---|---|
| 0 | 0 | 0 | 0 |
| 18 | 10.737 | 8.9861 | 10.438 |
| 36 | 10.065 | 10.971 | 9.7433 |
| 54 | 8.8196 | 10.161 | 9.0945 |
| 72 | 7.9016 | 8.4573 | 8.4890 |
| 90 | 8.3115 | 6.6686 | 7.9238 |

**Table 4.25 Comparison of the experimental data with the model at 4wt% nitric acid for the xylose released**

| Time (min) | Experimental Data (mg/ml) | Saeman's Model (mg/ml) | Two-fraction model (mg/ml) |
|---|---|---|---|
| 0 | 0 | 0 | 0 |
| 18 | 10.491 | 8.9861 | 10.438 |
| 36 | 9.7377 | 10.971 | 9.7435 |
| 54 | 8.9016 | 10.161 | 9.0947 |
| 72 | 8.6557 | 8.4573 | 8.4891 |
| 90 | 7.9016 | 6.6686 | 7.9239 |

**Table 4.26: Comparison of the experimental data withthe model at 5wt% nitric acid for the xylose released**

| Time (min) | Experimental Data (mg/ml) | Saeman's Model (mg/ml) | Two-fraction model (mg/ml) |
|---|---|---|---|
| 0 | 0 | 0 | 0 |
| 18 | 8.9016 | 7.5471 | 8.6872 |
| 36 | 7.5736 | 8.5833 | 7.5865 |
| 54 | 6.0656 | 7.3292 | 6.6252 |
| 72 | 5.8197 | 5.5688 | 5.7857 |
| 90 | 5.3934 | 3.9710 | 5.0526 |

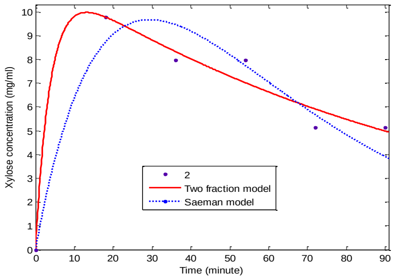

Figure 4.6 The graph for xylose released at 1wt% nitric acid

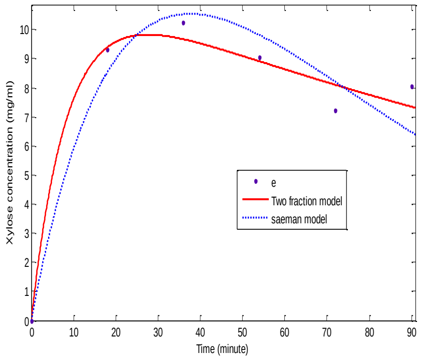

Figure 4.7 The graph for xylose released at 2wt% nitric acid

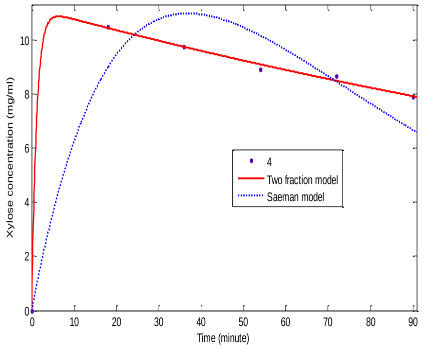

Figure 4.8 The graph for xylose released at 3wt% nitric acid

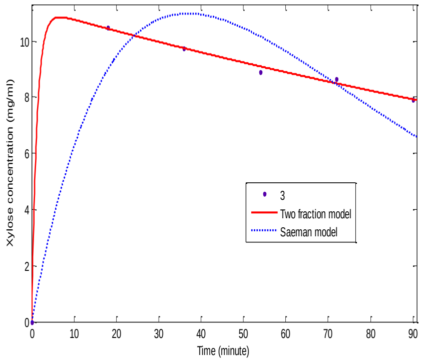

Figure 4.9 The graph for xylose released at 4wt% nitric acid

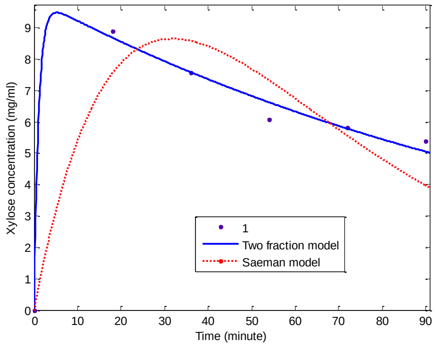

Figure 4.10 The graph for xylose released at 5wt% nitric acid

## 4.2 RESULTS AND DISCUSSION

Table 4.1 show the result of proximate analysis of the corn cob used in this study, this analysis shows that it is richer in hemicellulose than cellulose.

The experimental results of xylose concentrations are given respectively in Tables 4.3, 4.4, 4.5, 4.6 and 4.7, for phosphoric acid and Tables 4.15, 4.16, 4.17, 4.18, and 4.19 for nitric acid, which were converted from absorbance (nm) to concentration (mg/ml) with the aid of calibration data given in Table 4.2. Also, the experimental data were fit to Saeman's model and Two-fraction model.

The data of Table 4.2 was used to obtain the standard calibration curve used for the conversion of the absorbance data (nm) to concentration data (mg/ml), with the help of equation 4.1 showing the relationship between the two variables.

$$\text{Concentration} = \frac{\text{Absorbance}}{0.0061} \qquad (4.1)$$

Equation (4.1) was used to convert absorbance reading in column four of Table 4.3, 4.4, 4.5, 4.6 and 4.7 for phosphoric acid and Tables 4.15, 4.16, 4.17, 4.18, and 4.19 for nitric acid respectively to concentration in column five of the same tables.

Equation 4.2 is the general Saeman's model equation whereas equations 4.3 and 4.4 are Saeman model used for phosphoric and nitric acids hydrolysis respectively, to yield xylose.

$$C_B(t) = \frac{\mathrm{CAoK_1}}{(\mathrm{k_2-k_1})}\left[\mathrm{e^{-k_1t} - e^{-k_2t}}\right] \qquad (4.2)$$

$$\mathrm{X(t)} = \frac{14.6451\mathrm{K_1}}{(\mathrm{k_2-k_1})}\left[\mathrm{e^{-k_1t} - e^{-k_2t}}\right] \ (\mathrm{H_3PO_4}) \quad (4.3)$$

$$\mathrm{X(t)} = \frac{19.49\mathrm{K_1}}{(\mathrm{k_2-k_1})}\left[\mathrm{e^{-k_1t} - e^{-k_2t}}\right] \quad (\mathrm{HNO_3}) \ (4.4)$$

Xylose concentrations(mg/ml) were plotted for phosphoric acid from Table 4.3, 4.4, 4.5, 4.6 and 4.7, and for nitric acid from Tables 4.15, 4.16, 4.17, 4.18 and 4.19 respectively, against time (min), the experimental data were fit to equation (4.3) for phosphoric acid and equation (4.4) for nitric acid with curve fitting tool in MatLab software to obtain kinetic parameters ($\mathrm{k_1}$ *and* $\mathrm{k_2}$) and statistical parameter (Adjusted $\mathrm{R^2}$) as shown in Tables 4.8 and 4.20. The figures for the plots are shown in Figures 4.1, 4.2, 4.3, 4.4 ,4.5, 4.6, 4.7, 4.8, 4.9 and 4.10, for both phosphoric and nitric acids respectively. The values of $k_1$ and $k_2$ were substituted into equation 4.3 and 4.4 to generate Seaman's model data at different concentrations of phosphoric and nitric acids, given in column three of Tables 4.10, 4.11, 4.12, 4.13 and 4.14 for phosphoric acid and Tables 4.22, 4.23, 4.24, 4.25 and 4.26 for nitric acid, respectively.

Equation 4.4 is the general Two-fraction model equation whereas equations 4.6 and 4.7 are Two-fraction model used for phosphoric and nitric acids hydrolysis respectively, to yield xylose

$$C_B(t) = \frac{\mathrm{CAo\alpha K_1}}{(\mathrm{k_2-k_1})}\left[\mathrm{e^{-k_1t} - e^{-k_2t}}\right] \quad (4.5)$$

$$\mathrm{X(t)} = \frac{14.6451\alpha\mathrm{K_1}}{(\mathrm{k_2-k_1})}\left[\mathrm{e^{-k_1t} - e^{-k_2t}}\right] (\mathrm{H_3PO_4}) \ (4.6)$$

$$\mathrm{X(t)} = \frac{19.49\alpha\mathrm{K_1}}{(\mathrm{k_2-k_1})}\left[\mathrm{e^{-k_1t} - e^{-k_2t}}\right] \quad (\mathrm{HNO_3}) \ (4.7)$$

Xylose concentrations(mg/ml) were plotted from Table 4.3, 4.4, 4.5,4.6 and 4.7 for phosphoric acid and Tables 4.15, 4.16, 4.17, 4.18, and 4.19 for nitric acid respectively against time (min), the experimental data were fit to equation (4.6) for phosphoric acid and equation (4.7) for nitric acid with curve fitting tool in MatLab to obtain kinetic parameters ($\mathrm{k_1}$ *and* $\mathrm{k_2}$), $\propto$ and statistical parameter(Adjusted $\mathrm{R^2}$), as shown in Table 4.9 and 4.21. The figures for the plots are shown in Figures 4.1, 4.2, 4.3, 4.4, 4.5 ,4.6, 4.7, 4.8, 4.9 and 4.10, for both phosphoric and nitric acids respectively. The values of $k_1$, $k_2$ and$\propto$were substituted into equation 4.6 and 4.7 to generate Two-fraction model data at different concentrations of phosphoric acid and nitric acids, given in column four of Tables 4.10, 4.11, 4.12, 4.13 and 4.14 for phosphoric acid and Tables 4.22, 4.23, 4.24, 4.25 and 4.26 for nitric acid, respectively.

In a first approach the model of seaman was applied to model xylose concentration. The result of fitting by the Saeman's model (Table 4.8) were unsatisfactory mainly showing the values of the statistical parameter (Adjusted $\mathrm{R^2} < 0.9$) as were also observed by Antonio *et al.*, [18], Onyelucheya *et al.*, [4], Soleimani *et al.*, [15] and Yuan *et al.*, [1]in their research works.

In a second approach the two fraction model was applied (Table 4.9) showing (Adjusted $\mathrm{R^2}$) closer to one in line with the research work of Aguilar et al., [14], Antonio et al., [18], Wang *et al.*, [13] and Yuan *et al.*, [1].

Comparing the values of kinetic parameter ($k_1 and k_2$) it can be observed that the kinetic coefficients of generation reaction of xylose are higher than those of the degradation reaction.
The values of ∝ was in the range 0.5-0.8 mg/mg, the average 0.7 mg/mg indicating 70% susceptibility to hydrolysis which is in line with the values reported by previous researchers. For example, Kim & Lee [19] reported values of ∝ in the range 0.58-0.80 g/g for oak hydrolysis. Eken-Saracglu et al., [9] found values of 0.84 g/g for corn cob and 0.86 g/g for sunflower seed hulls, which were also reported by Negahdar*et al*., [20] and Delbecq *et al*., [21].

The fitting of experimental data using the Saeman's model (Table 4.20) was not successful as compared with the Two-fraction model (Table 4.21) which gave a better fit this is based on the statistical parameter (Adjusted $R^2$) obtained. The fractional value ∝ varied from 0.4 – 0.5 with an average value of 0.51 mg/mg indicating an average of 51% susceptibility.
$K_1$ was observed to be increasing as acid concentration increases. This means that xylose yield increased with acid concentration, corroborating the findings of Onyelucheya *et al*., [4] and Wan *et al*. [7].

To substantiate the fact that the Two-fraction model is better compared to the Saeman's model, from Tables 4.10, 4.11, 4.12, 4.13, 4.14, 4.22, 4.23, 4.24, 4.25 and 4.26, comparing their third column (Saeman's model) with the fourth column (Two-fraction model) of the same Tables, the values from the fourth column are almost always closer to the experimental values.

Using the Two fraction model which gave a better fit over Saeman's model, the optimum using phosphoric acid as a catalyst for xylose was predicted as 3wt% $H_3PO_4$ for 38mins, which gave 11.034 mg/ml with 67% susceptibility to hydrolysis.Whereas the maximum production using nitric acid as a catalyst for xylose was predicted at 3wt% $HNO_3$ for 6mins, which gave 10.859 mg/ml with 52% susceptibility to hydrolysis.

Comparing these results with the maximum production obtained by Laboratory confirmation test; using phosphoric acid the confirmation result at 3wt% $H_3PO_4$ for 38mins gave 9.754mg/ml. Whereas using nitric acid as a catalyst for xylose production at 3wt% $HNO_3$ for 6mins gave 8.298 mg/ml of xylose. And comparing these results with the maximum production obtained by Laboratory confirmation test and previous researchers; Antonio *et al*., [18] in their study of hydrolysis of sugarcane bagasse using nitric acid, the maximum conditions selected were 122°C, 6wt% and 9.3mins which gave 18.6mg/ml of xylose, similar to the conditions and result of Liu *et al*., [22].

Sara *et al.,* [16] Studied the hydrolysis of sugar cane bagasse using phosphoric acid, the maximum conditions selected at 122°C, 4w% and 300mins, which gave 17.6mg/ml of xylose, and Soleimani *et al*., [15] confirmed these conditions and result in their recent research.
Esther *et al*., [10], in their study on the acid hydrolysis of wheat straw using sulphuric acid as a catalyst, the maximum conditions selected were 2wt% of $H_2SO_4$ at 130°c for 29mins, which gave xylose concentration of 18.9mg/ml with 59% susceptibility. And Onyelucheya *et al*., [4] in their acid hydrolysis of cassava peel using phosphoric acid, found the maximum xylose concentration as 33mg/ml at 10wt%, 3mins and 121°C.

## CONCLUSSION

This work will help to add knowledge and elucidate the kinetics of the acid hydrolysis of corn cob to yield xylose. The research has shown that corn cob is richer in hemicellulose content than cellulose, favoring the yield of xylose. Again, it has been shown that the rate of decomposition of the polymer ($K_1$) is greater than the rate of degradation of the monomer ($K_2$). Two-fraction model is found to be a better model for fitting of the hydrolysis data, as it gave better fits over the Seaman's model, and the parameter ∝ is less than or equal to 1 and is slightly affected by increase in acid concentration.

A maximum concentration of 11.034mg/ml of xylose was produced when 3wt% $H_3PO_4$ was used as catalyst for the hydrolysis and at a time interval of 38mins, with 67% susceptibility to hydrolysis, whereas for the nitric acid hydrolysis, 0.054mg/ml maximum glucose concentration was produced using 2wt% of the nitric acid, at a time interval of 77mins, with 0.6% susceptibility to hydrolysis. And comparing the results obtained using phosphoric acid and nitric acid, it has been established that the nitric acid is a more efficient catalyst for the hydrolysis. Also, the results obtained from this research within the already established operational conditions shows that corn cob as a lignocellulosic material is suitable for the production of xylose.

## REFERENCES

[1] Yuan, Q., Liu, S., Ma M., Ji X., Choi S. and Si C. 2021. The kinetics studies on hydrolysis of hemicellulose. Frontiers in Chemistry; 9:781291.

[2] Garrote, G., Dominguez, H., Parajo, J.C. 2001. Kinetic modeling of corn cob auto hydrolysis. Process Biochemistry 36: 571-578.

[3] Jin, L.Q., Zhao, N., Liu, Z.Q., Liao, C.J., Zheng X.Y., Zheng Y.G. 2018. Enhanced production of xylose from corncob hydrolysis with oxalic acid as catalyst. Bioprocess Biosyst Eng, 41: 57-64.

[4] Onyelucheya O.E., Nwabanne J.T, Onyelucheya C.M. and Adeyemo O.E. 2016. Acid Hydrolysis of Cassava Peel. International Journal of Scientific & Technology Research, 5(1): 184-187.

[5] Kalyani D.C., Fakin T., Horn S.J., Tschentscher R. 2017. Valorization of woody biomass by combining enzymatic saccharification and pyrolysis. Green Chem, 19:3302–3312.

[6] Guo Z., Ling Z., Wang C., Zhang X. and Xu F. 2018. Integration of facile deep eutectic solvents pretreatment for enhance denzymatic hydrolysis and lignin valorization from industrial xylose residue. Bioresource Technol, 265:334–339.

[7] Wan L., Gao Z., Wu B., Cao F., Jiang M., Wei P. 2021. Hydrolysis of Corncob Hemicellulose by Solid Acid Sulfated Zirconia and its Evaluation in Xylitol Production. Appl. Biochem. Biotechnol, 193 (1), 205–217.

[8] Saeman, J.F. 1945. Kinetics of wood saccharification. Hydrolysis of cellulose and decomposition of sugars in dilute acid at high temperature. Industrial and Engineering Chemistry, 37, 43–52.

[9] Eken-Saraçoğlu N., Mutlu S.F., Dilmaç G. and Çavuşoğlu H. 1998. A comparative kinetic study of acidic hemicellulose hydrolysis in corn cob and sunflower seed hull. Bio-resource Technology, 65 (1-2): 29-33.

[10] Esther, G.R., Oscar, M.P., Lorenzo, J.E., Jose, A.R. and Manuel V. 2012. Acid Hydrolysis of Wheat Straw: A kinetic Study, Biomass and Bio-energy, 36, 346-35.

[11] Liang C., Hu Y., Guo L., Wu L., Zhang W. 2017. Kinetic study of acid hydrolysis of corncobs to levulinic acid. Bio Resources; 12(2), 4049-4061.

[12] da Costa Lopes A.M., Łukasik R.M. 2018. Separation and Recovery of a Hemicellulose-Derived Sugar Produced from the Hydrolysis of Biomass by an Acidic Ionic Liquid. Chem Sus Chem, 11 (6): 1099-1107.

[13] Wang, C., Yang, G., Zhang, X., Shao, L., Mao J., Liu S. and Xu F. 2019, A kinetic study on the hydrolysis of corncob residues to levulinic acid in the FeCl3-NaCl system. Springer-Cellulose 26:8313-8323.

[14] Aguilar, R., Ramirez, J.A., Garrote, G., Va´zquez M. 2002. Kinetic study of the hydrolysis of sugar cane bagasse. Journal of Food Engineering. 55:309-318.

[15] Soleimani, M.,Tabil, L. G. Panigrahi, S. 2018. A Kinetic Study of Xylose Recovery from a Hemicellulose-Rich Biomass for Xylitol Fermentative Production. Chem. Eng. Commun. 206 (2), 193206.

[16] Sara Ga´mez, Juan Jose Gonza´lez-Cabriales, Gil Garrote B. and Manuel Va´zquez. 2006. Study of the hydrolysis of sugarcane bagasse using phosphoric acid. Journal of Food Engineering 74: 78–88.

[17] Lavarack B.P., Griffin G.J. and Rodman D. 2002. The Acid Hydrolysis of Sugarcane Bagasse Hemicellulose to Produce Xylose, Arabinose and other Products, Biomass and Bio-energy, 23, 367-380.

[18] Antonio R.C., Jose A.R., Gril G., Manuel V. 2004. Hydrolysis of Sugarcane Bagasse using Nitric Acid: A Kinetic Assessment, Journal of Food Engineering, 61, 142-152,

[19] Kim S.B. and Lee Y.Y. 1987. Kinetics in acid-catalyzed hydrolysis of hardwood hemicellulose. Biotechnology Bioengineering Symposium, 17, 71–84.

[20] Negahdar L., Delidovich I. and Palkovits R. 2016. Aqueous-phase Hydrolysis of Cellulose and Hemicelluloses over Molecular Acidic Catalysts: Insights into the Kinetics and Reaction Mechanism. Appl. Catal. B: Environ. 184, 285–298.

[21] Delbecq, F., Wang, Y., Muralidhara, El-Ouardi A. K., El-Ouardi K., Marlair G. and Len C. 2018. Hydrolysis of Hemicellulose and Derivatives-A Review of Recent Advances in the Production of Furfural. Front. Chem. 6, 146.

[22] Liu F., Xu W.F., Mu H., Lv Z.R., Peng J., Guo C. 2020. Inhibition Kinetics of

Acetosyringone on Xylanase in Hydrolysis of Hemicellulose. Biosci. Biotechnol. Biochem. 84 (9), 1788-1798.

[23] Alessandra V., Isabella D.B., Emanuele R. and Vincenza C. 2012. Hydrolysis of Lignocellulosic Biomass Current Status of Processes and Technologies and Future Perspectives, Bioethanol, Marco Aurelio Pinheiro Lima (Ed.), ISBN: 978-953-51-008-9.

[24] Agarry, S.E., Ajani, A.O., Agbede, O.O. 2011. A Comparative Kinetic Study of Acidic Hydrolysis of Wastes Cellulose from Agricultural Derived Biomass, Journal of Applied Science and Environmental Management, 15, 531-537.

[25] Arun, B., Bahl, B.S. 2010. A Textbook of Organic Chemistry, 19th Revised Edition, S. Chad and Company Ltd, PP. 638-641.

[26] Andérez Fernández M., Rissanen J., Pérez Nebreda A., Xu C., Willför S., García Serna J. 2018. Hemicelluloses from Stone pine, Holm Oak, and Norway spruce with Subcritical Water Extraction – Comparative Study with Characterization and Kinetics. J. Supercrit. Fluids 133, 647–657.

[27] Bader S. and James D. 2013. Results from the Xylitol for Adult Caries Trial (X-ACT) . The Journal of the American Dental Association. 144 (1) 21–30.

[28] Converti, A., Parego, P., Dominguez, J.M. 1999. Xylitol Production from Hardwood Hemicellulose Hydrosylates (PDF). Applied Biochemistry and Biotechnology. 82: 141–151.

[29] Herrera, A., Te´llez-Luis S.J. and Va´zquez M. 2003. Production of xylose from sorghum straw using hydrochloric acid. J Cereal Sci. 37(3): 267-74.

[30] Islam S.M.R., Mimi Sakinah A.M. 2011. Kinetic Modeling of the Acid Hydrolysis of Wood Sawdust. International Journal of Chemical and Environmental Engineering, 2(5): 333-337.

[31] Jeevan, P., Nelson, R., Edith, R. 2011. Optimization studies on acid hydrolysis of corn cob hemicellulosichydrolysate for microbial production of xylitol. Journal of microbiology and biotechnology research (4), 114-123.

[32] Kapu, N.S., Yuan, Z., Chang, X.F., Beatson, R., Martinez D.M. and Trajano H.L. 2016. Insight into the Evolution of the Proton Concentration during Auto hydrolysis and Dilute-Acid Hydrolysis of Hemicellulose. Biotechnol. Biofuels 9, 224.

[33] Neureiter, M., Danner, H., Thomasser, C., Saidi, B., Braun, R. 2002. Dilute acid hydrolysis of sugar cane bagasse at varying conditions. Appl. Biochem. Biotechnol. 98: 49-58.

[34] Nigam, P., Singh, D. 1995. Processes for Fermentative Production of Xylitol- a Sugar Substitute. Process Biochemistry. 30: 117–124.

[35] Nguyen, Q.A., Tucker, M.P., Keller, F.A. and Eddy F.P. 2000. Two-stage dilute acid pretreatment of softwoods. Applied Biochemistry Biotechnology; 84-86:561-576.

[36] Rodrı´guez-Chong A., Ramı´rez J.A., Garrote G. and Va´zquez M. 2004. Hydrolysis of sugar cane bagasse using nitric acid: a kinetic assessment. Journal Food Engineering; 61(2):143-52.

[37] Sánchez, O.J. , Cardona, C.A. 2008. Trends in biotechnological production of fuel ethanol from different feed stocks, Bioresource Technology 99, 5270-5295.

[38] Santos, V. T. d. O., Siqueira G., Milagres A. M. F., Ferraz, A. 2018. Role of Hemicellulose Removal during Dilute Acid Pretreatment on the Cellulose Accessibility and Enzymatic Hydrolysis of Compositionally Diverse Sugarcane Hybrids. Ind. Crops Prod. 111, 722–730.

[39] Shi, S., Guan, W., Kang, L., Lee, Y.Y. 2017. Reaction Kinetic Model of Dilute Acid-Catalyzed Hemicellulose Hydrolysis of Corn Stover under High-Solid Conditions. Ind. Eng. Chem. Res. 56 (39), 10990–10997.

[40] Va´zquez M., Oliva M., Te´llez-Luis S.J., Ramı´rez J.A. 2007, Hydrolysis of sorghum straw using phosphoric acid: evaluation of furfural production. Bioresource Technology; 98:305360.

[41] Wang, Y., Cao, X., Zhang, R., Xiao, L., Yuan, T., Shi Q. 2018. Evaluation of Xylo-oligosaccharide Production from Residual Hemicelluloses of Dissolving Pulp by Acid and Enzymatic Hydrolysis. RSC Adv. 8 (61), 35211–35217.

[42] Xu, F., Shi, Y.C., Wu, X.R., Theerarattananoon K., Staggenborg S., Wang D.H. 2011. Sulphuric acid pretreatment and enzymatic hydrolysis of photoperiod sensitive sorghum for ethanol production. Bioprocess Biosystems Engineering; 34(4):48592.

[43] Zhu S., Wu Y., Yu Z., Zhang X., Wang C. and Yu F. 2006. Production of ethanol from microwave-assisted alkali pretreated wheat straw. Process Biochemistry; 41(4):869e73.

*All © 2022 are reserved by International Journal of Advanced Science and Engineering. This Journal is licensed under a Creative Commons Attribution-Non Commercial-ShareAlike 3.0 Unported License.*